NeuroImage: Clinical 19 (2018) 625–632

Contents lists available at ScienceDirect

NeuroImage: Clinical

journal homepage: www.elsevier.com/locate/ynicl

Hypometabolism of the posterior cingulate cortex is not restricted to Alzheimer's disease

Nienke M.E. Scheltens[a,*], Kars van der Weijden[b], Sofie M. Adriaanse[b], Danielle van Assema[b], Priscilla P. Oomen[a], Welmoed A. Krudop[a], Adriaan A. Lammertsma[b], Frederik Barkhof[b,c], Teddy Koene[d], Charlotte E. Teunissen[e], Philip Scheltens[a], Wiesje M. van der Flier[a,f], Yolande A.L. Pijnenburg[a], Maqsood Yaqub[b], Rik Ossenkoppele[a], Bart N.M. van Berckel[b]

[a] Alzheimer Center and Department of Neurology, Neuroscience Campus Amsterdam, VU University Medical Center, Amsterdam, The Netherlands
[b] Department of Radiology and Nuclear Medicine, Neuroscience Campus Amsterdam, VU University Medical Center, Amsterdam, The Netherlands
[c] Institutes of Neurology and Healthcare Engineering, UCL, London, UK
[d] Alzheimer Center and Department of Medical Psychology, VU University Medical Center, Amsterdam, The Netherlands
[e] Neurochemistry Laboratory and Biobank, Department of Clinical Chemistry, Neuroscience Campus Amsterdam, VU University Medical Center, Amsterdam, The Netherlands
[f] Department of Epidemiology and Biostatistics, VU University Medical Center, Amsterdam, The Netherlands

ARTICLE INFO

Keywords:
Alzheimer's disease
Frontotemporal dementia
Posterior cingulate cortex
[^{18}F]FDG-PET
Hypometabolism

ABSTRACT

When differential diagnosis of dementia includes both Alzheimer's disease (AD) and the behavioural variant of frontotemporal dementia (bvFTD), distribution of cerebral glucose metabolism as measured using [^{18}F]-2-fluoro-2-deoxy-D-glucose positron emission tomography ([^{18}F]FDG-PET) may be helpful. One important clue for differentiation is the presence of hypometabolism in the posterior cingulate cortex (PCC), usually associated with AD. PCC hypometabolism however, could also be present in bvFTD. Therefore, the specificity of PCC hypometabolism was examined. Based on visual reading PCC hypometabolism was present in 69–73/81 probable AD patients, in 10–16/33 probable bvFTD patients, and in 0–1/22 cognitive normal (CN) subjects. Findings were validated using a PCC to reference tissue [^{18}F]FDG standard uptake value ratio (SUVr) cut-off, which was derived from the receiver operating characteristic (ROC) separating probable AD from CN, resulting in 9–14/33 bvFTD patients having PCC hypometabolism, depending on the reference tissue used. In conclusion, PCC hypometabolism is not restricted to AD.

1. Introduction

Reduced uptake of [^{18}F]-2-fluoro-2-deoxy-D-glucose ([^{18}F]FDG) in the posterior cingulate cortex (PCC) is a characteristic feature of Alzheimer's disease (AD)(Herholz, 2014; Kato et al., 2016; Landau et al., 2011; Minoshima et al., 1997). However, PCC hypometabolism may not be restricted to AD and can also be seen in other dementias such as the behavioural variant of frontotemporal dementia (bvFTD), which is characterized by most prominent hypometabolism in the frontal lobe (Diehl et al., 2004). Previous studies reported inconsistent findings regarding involvement of the PCC in bvFTD, and involvement of the PCC mostly coincided with more advanced stages of the disease (Broe et al., 2003; Diehl-Schmid et al., 2007; Ishii et al., 1998; Kato et al., 2016; Whitwell et al., 2004). Little is known about the prevalence of PCC hypometabolism at time of bvFTD diagnosis, nor about its association with clinical phenotype. The aim of this study was therefore to assess the prevalence of PCC hypometabolism in AD, bvFTD, and cognitive normal (CN) subjects using visual reading. A second objective was to explore associations between PCC standard uptake value ratio (SUVr; using both cerebellum and pons as reference regions) and clinical characteristics.

2. Methods

2.1. Subjects

A total of 136 subjects from the Amsterdam dementia cohort were included(van der Flier et al., 2014). AD subjects (n = 81) met clinical criteria for probable AD and had CSF tau/Aβ_{1-42} > 0.52, implying high likelihood for underlying AD pathology (Duits et al., 2014;

* Corresponding author at: De Boelelaan 1118, 1081 HZ Amsterdam, The Netherlands.
E-mail address: n.scheltens@vumc.nl (N.M.E. Scheltens).

https://doi.org/10.1016/j.nicl.2018.05.024
Received 24 December 2017; Received in revised form 18 April 2018; Accepted 19 May 2018
Available online 22 May 2018

Mckhann et al., 2011). BvFTD subjects (n = 33) met clinical criteria for probable bvFTD and diagnosis was confirmed by a neurologist specialised in bvFTD (YP) (Rascovsky et al., 2011). Furthermore, all bvFTD patients had CSF $A\beta_{1-42}$ > 550 pg/mL, implying a low likelihood for underlying amyloid pathology (Mulder et al., 2010). CN subjects (n = 22) performed normally on an extensive neuropsychological test battery, and showed no abnormalities on MRI indicative of underlying neurodegeneration, as evaluated by an experienced neuroradiologist (FB). All CN subjects had CSF tau/$A\beta_{1-42}$ < 0.52, implying a low likelihood for underlying AD pathology (Duits et al., 2014). The local Medical Ethics Review Committee approved the study. All subjects provided written informed consent prior to inclusion.

2.2. Neuropsychological assessment

A standard neuropsychological test battery was used to assess major cognitive functions (van der Flier et al., 2014). Test scores were transformed into z-scores, and inverted where appropriate, so that higher scores represented better performances. Compound scores were calculated for each cognitive domain investigated. In addition, Mini-Mental State Examination (MMSE), Clinical Dementia Rating scale (CDR), and Neuropsychiatric Inventory (NPI) were included.

2.3. APOE genotype and CSF biomarkers

Collection and analysis of APOE genotype and CSF biomarkers were performed as described previously (van der Flier et al., 2014). For inclusion of bvFTD subjects, the cut-off for normal CSF $A\beta_{1-42}$ was set at > 550 pg/mL. For inclusion of AD patients, the cut-off for abnormal CSF tau/$A\beta_{1-42}$ was set at > 0.52, and for CN subjects < 0.52 (Duits et al., 2014). Finally, associations between CSF biomarkers and PCC SUVr were assessed using continuous variables.

2.4. MRI protocol

T1-weighted 3D MPRAGE images were acquired for co-registration, segmentation, and region of interest definition. Images were obtained on a 1.5 T Sonata scanner (Siemens, Erlangen, Germany; slice thickness 1.5 mm, 160 slices, matrix size 256 × 256, voxel size 1 × 1 × 1.5 mm, echo time 3.97 ms, repetition time 2700 ms, flip angle 8°) or a 3 T SignaHDxt scanner (General Electric, Milwaukee, Wisconsin, USA; slice thickness 1 mm, 180 slices, matrix size 256 × 256, voxel size 1x1x1.5 mm, echo time 3 ms, repetition time 708 ms, flip angle 12°).

2.5. PET protocol

Prior to injection of ~185 MBq [^{18}F]FDG, patients were required to rest for 10 min with eyes closed and earplugs in a dimly lit room. [^{18}F]FDG PET emission scans were acquired at 45 min post injection using either an ECAT EXACT HR + (Siemens/CTI, Knoxville, TN) or a Gemini TF-64 PET/CT (Philips, Best, The Netherlands) scanner. In addition, in case of the HR +, a 10 min transmission scan or, in case of the Gemini, a low dose CT scan was acquired prior to the emission scan to correct emission data for tissue attenuation. Image acquisition, pre-processing and the reconstruction protocol have been described elsewhere (Verfaillie et al., 2015).

2.6. Imaging analysis

T1 weighted MR images were co-registered to corresponding [^{18}F]FDG PET data using the Vinci software package (version 2.56.0). Using PVElab together with the Hammers template, regions of interest (ROI) were delineated on the MRI scans and superimposed onto the dynamic PET scan to generate regional time activity curves (TAC). (Hammers et al., 2002; Svarer et al., 2005) Since the pons is not a standard region in this template, it was delineated manually on the co-registered T1w MR image using in-house built software in IDL, and superimposed onto the dynamic PET images. The manual delineation was performed based on voxel intensity differences between the pons and the remaining part of the brainstem on the T1w MR image. Using SPM segmentation, pons white matter volumes were extracted from which a 95% CI of pons white matter volume was calculated for quality insurance of the manual delineation. Outliers were checked on both their delineation and segmentation, and when necessary corrected. PCC SUVr was calculated as PCC to reference region ratio, by dividing the images by the reference region value. For the reference tissue cerebellum grey matter (further referred to as 'cerebellum') and pons white matter (further referred to as 'pons') TACs were assessed separately.

Two nuclear medicine physicians, blinded for clinical diagnosis, performed visual reading. The level of experience in visual reading of [^{18}F]FDG brain images differed between readers. Reader A was very experienced, reading multiple [^{18}F]FDG images weekly, whilst reader B recently completed training to be nuclear medicine physician. PCC hypometabolism was considered to be present when the PCC (defined using anatomical boundaries that are described elsewhere (Minoshima et al., 1994)) was isointense – since healthy brain metabolism is associated with highest glucose uptake in the PCC (Loessner et al., 1995) – or hypointense compared with other cortical regions by thresholding the SUVr image to identify the area in the brain with the highest activity concentration (Minoshima et al., 1997).

2.7. Statistical analyses

Statistical analyses were performed using SPSS for Windows version 22.0 (IBM Corp. Armonk, NY). Clinical characteristics were compared between diagnostic groups (AD, bvFTD and CN) using chi-square tests (sex, APOE genotype), Kruskal-Wallis analyses (education, duration of complaints, MMSE, CDR, and NPI), or analysis of variance (ANOVA) with post hoc Bonferroni analyses (SUVr, age, age at onset of complaints, CSF biomarkers, neuropsychological compound z-scores). When group differences were observed with chi-squared tests or Kruskal-Wallis analyses, ANOVA with Tamhane's T2 post hoc analyses was used, in which equal variances are not assumed.

For assessment of PCC hypometabolism prevalence in AD, bvFTD and CN, first visual reading was performed. Inter-reader agreement was assessed using Cohen's kappa (κ). Agreement was considered poor if $\kappa < 0.20$, satisfactory if $0.21 < \kappa < 0.40$, moderate if $0.41 < \kappa < 0.60$, good if $0.61 < \kappa < 0.80$, and excellent if $\kappa > 0.81$ (Zwan et al., 2014).

Second, the presence of PCC hypometabolism in bvFTD was verified using a SUVr cut-off, which was defined based on the Receiver Operating Characteristic (ROC) separating AD from CN. Findings were validated using the split-half approach, in which the sample was randomly split in half, resulting in a training sample and test sample. In addition, ROC analyses were performed separating AD from bvFTD, and separating bvFTD from CN. Since we aimed to explore specificity of PCC hypometabolism, we chose cut-offs corresponding with a minimum specificity of 90%. Furthermore, ROC curves of cerebellum-normalised SUVr were compared with ROC curves of pons-normalised SUVr with the method by Hanley and McNeil (1983) using MedCalc Statistical Software version 18.2.1 (MedCalc Software bvba, Ostend, Belgium; https://www.medcalc.org; 2016).

Relationships between PCC [^{18}F]FDG SUVr (dependent variable) and all clinical characteristics shown in Table 1 (independent variables) were explored using linear regression analyses. Age, sex, diagnostic group and scanner type were included as covariates. In addition, the interaction between diagnosis and clinical variable of interest was introduced into the model.

Within the bvFTD group we compared characteristics of patients having normal PCC metabolism with patients having PCC hypometabolism based on visual reading (reader A). First, clinical characteristics were compared between these two subgroups using chi-squared tests,

Table 1
Cohort characteristics.

	n = 136	AD n = 81	bvFTD n = 33	CN n = 22
PCC metabolism				
[^{18}F]FDG SUVr cerebellum	136	1.04 ± 0.11$^{\dagger\|}$	1.13 ± 0.15§	1.21 ± 0.12
[^{18}F]FDG SUVr pons	136	1.50 ± 0.18$^{\dagger\|}$	1.64 ± 0.19	1.73 ± 0.19
Demographics				
Age	136	63 ± 8	65 ± 8	61 ± 8
Female	136	30(37)	13(39)	6(27)
Education	135	5.2 ± 1.2	4.6 ± 1.4§	5.6 ± 1.1
Duration of complaints	129	3.3 ± 2.3	3.9 ± 3.2	3.3 ± 1.7
Age at onset complaints	129	60 ± 8	61 ± 7	57 ± 9
APOE genotype				
APOE e4 positive	125	45 (56)$^{\S\|}$	7 (21)	7 (32)
CSF				
Abeta$_{1-42}$ pg/mL	136	473 ± 115$^{\dagger\|}$	942 ± 237	993 ± 203
tau pg/mL	136	692 ± 401$^{\dagger\|}$	350 ± 199	262 ± 141
ptau pg/mL	136	94 ± 2$^{\dagger\|}$	45 ± 16	51 ± 30
Neuropsychological compound z-scores				
Memory	136	−0.34 ± 0.73$^{\dagger\#}$	0.03 ± 0.65†	0.88 ± 0.78
Language	130	−0.16 ± 1.05‡	−0.13 ± 0.66$^{\#}$	0.58 ± 0.71
Attention	135	−0.13 ± 0.73§	−0.00 ± 0.87	0.36 ± 0.71
Visuospatial functioning	118	−0.22 ± 1.08	0.21 ± 0.49	0.28 ± 0.89
Executive functioning	135	−0.14 ± 0.79†	−0.17 ± 0.91‡	0.57 ± 0.74
MMSE	135	23 ± 4†	24 ± 3†	28 ± 3
CDR	90	0.8 ± 0.3	0.8 ± 0.5	0.6 ± 0.4*
NPI	104	9.6 ± 8.4¶	19.5 ± 14.6	16 ± 11*

Data are presented as mean ± standard deviation, or as number (percentage). APOE e4 positive genotype: ≥one e4 alleles. *Only available for 10/22 (CDR) or 12/22 (NPI) in CN subjects. Variables with significant differences based on chi-squared tests, Kruskal-Wallis analyses, or ANOVA are indicated as follows.

† Difference with CN $p \leq 0.001$.
‡ Difference with CN $p \leq 0.01$.
§ Difference with CN $p \leq 0.05$.
$^{\|}$ Difference with bvFTD $p \leq 0.001$.
¶ Difference with bvFTD $p \leq 0.01$.
$^{\#}$ Difference with bvFTD $p \leq 0.05$.

Kruskal-Wallis analyses, or ANOVA. In addition, regression analyses were repeated as described before, replacing the variable diagnostic group by PCC metabolism (normal metabolism versus hypometabolism based on visual reading by reader A) in the model. Statistical significance was set at $p < 0.05$. Due to the explorative character of our study (exploring associations between PCC metabolism and clinical characteristics), no statistical correction for multiple testing was performed.

3. Results

3.1. Cohort characteristics

Characteristics of the three diagnostic groups are summarised in Table 1.

3.2. Prevalence of PCC hypometabolism

Fig. 1 shows example [^{18}F]FDG PET scans of one subject from each diagnostic group. Using either cerebellum or pons as reference region, PCC SUVr was lower in AD than in bvFTD and CN, with the largest range of values in bvFTD (Fig. 2). Presence of PCC hypometabolism was assessed with visual reading by two nuclear medicine physicians. Results are shown in Table 2 together with corresponding Cohen's κ. Inter-reader agreement per subject is indicated by different colours in Fig. 2.

Presence of PCC hypometabolism in bvFTD was validated using an [^{18}F]FDG SUVr cut-off defined by the ROC separating AD from CN. When using cerebellum as reference region, the cut-off was set at 1.10 (area under the curve [AUC] = 0.86, specificity = 91%, sensitivity = 70%; Table 3, and Fig. 3). Based on this cut-off, 42% of bvFTD patients had PCC hypometabolism. When using pons as reference region, the cut-off was set at 1.52 (AUC = 0.81, specificity = 91%, sensitivity = 56%, Table 3, and Fig. 3). Using this cut-off, 27% of bvFTD patients had PCC hypometabolism. Split-half validation with cerebellum as reference region resulted in a SUVr cut-off at 1.03 (AUC = 0.85, specificity = 92%, sensitivity = 50%) in the training sample, corresponding with 40% of 15 bvFTD patients having PCC hypometabolism in the test sample. Split-half validation with pons as reference region resulted in a SUVr cut-off at 1.39 (AUC = 0.77, specificity = 92%, sensitivity = 19%) in the training sample, corresponding with 13% of 15 bvFTD patients having PCC hypometabolism in the test sample. Additional characteristics of ROC curves separating CN from bvFTD, and bvFTD from AD are shown in Table 3 and Supplementary figure. No differences were found when ROC-AUC from pons-normalised data were compared with cerebellum-normalised data using the method by Hanley and McNeil (1983).

3.3. Relationship between PCC metabolism and clinical characteristics in diagnostic groups

We performed age, sex, and scanner adjusted linear regression analyses to assess associations between PCC [^{18}F]FDG SUVr and demographics, neuropsychological, and neurobiological characteristics stratified for clinical diagnosis (with CN as reference group). When the cerebellum was used as reference region, there was a significant interaction between clinical diagnosis and age ($p_{interaction} = 0.007$, eta^2 = 0.125), showing a positive association between PCC metabolism and age in AD ($p_{interaction} = 0.047$, standardized beta [standardized error; SE] = 0.010[0.005]). A comparable effect was seen between clinical diagnosis and age at onset of complaints ($p_{interaction} = 0.015$, eta^2 = 0.119), showing a positive association between PCC metabolism and age at onset of complaints in AD as well ($p_{interaction} = 0.034$, standardized beta[SE] = 0.011[0.055]). Results are shown in Fig. 4. No associations were found when the pons was used as reference region for PCC [^{18}F]FDG SUVr.

3.4. Characteristics of bvFTD patients with PCC hypometabolism compared with bvFTD patients with normal PCC metabolism

Compared with bvFTD patients with normal PCC metabolism – as assigned based on visual reading by reader A – bvFTD patients with PCC hypometabolism had lower PCC [^{18}F]FDG SUVr (using cerebellum [$p = 0.001$] or pons [$p = 0.004$] as reference region), and performed worse on the memory domain ($p = 0.021$; data shown in Table 4).

3.5. Relationship between PCC metabolism and clinical characteristics in bvFTD patients

We performed age, sex, and scanner adjusted linear regression analyses to assess associations between PCC [^{18}F]FDG SUVr and demographics, neuropsychological, and neurobiological characteristics stratified for presence of PCC hypometabolism based on visual reading (reader A) in bvFTD patients. When the cerebellum was used as reference region, there was a positive association between PCC hypometabolism and visuospatial functioning ($p_{interaction} = 0.044$, eta^2 = 0.208, standardized beta[SE] = 0.163[0.075]). When the pons was used as reference region, there was a positive association between PCC hypometabolism and memory ($p_{interaction} = 0.002$, eta^2 = 0.419,

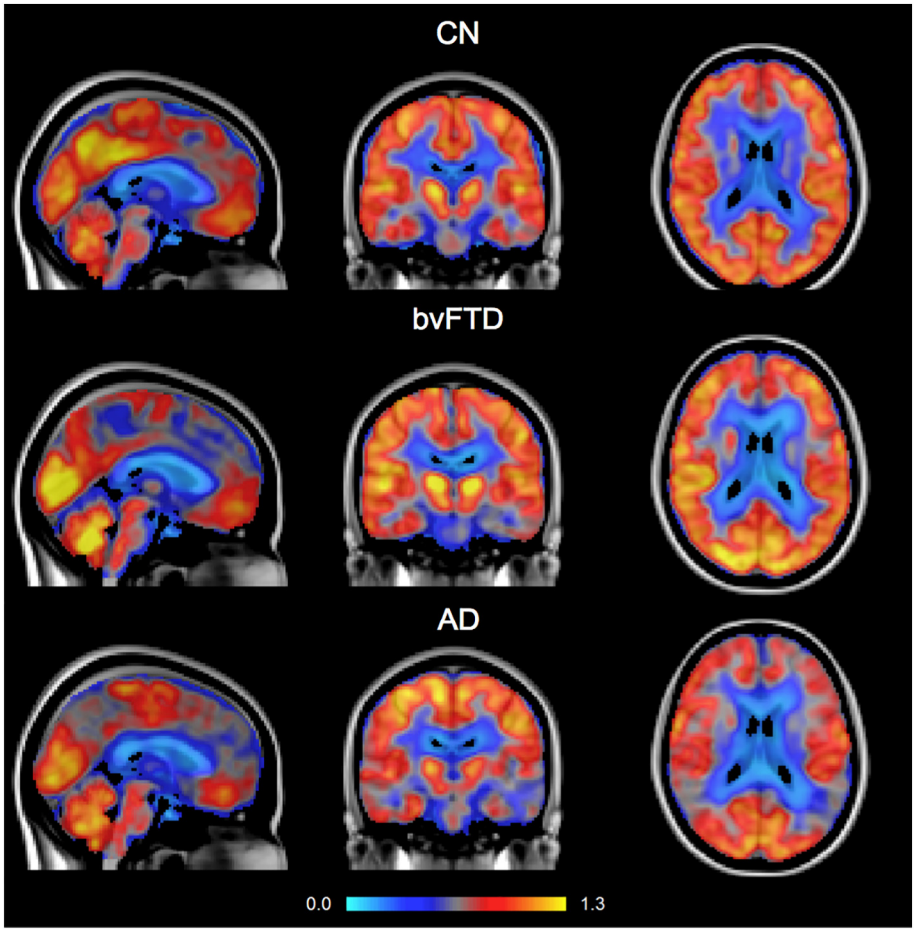

Fig. 1. PCC [^{18}F]FDG uptake visualised in a CN subject (SUVr = 0.948), a bvFTD patient (SUVr = 0.939), and an AD patient (SUVr = 0.768). SUVr were measured using the cerebellum as reference region.

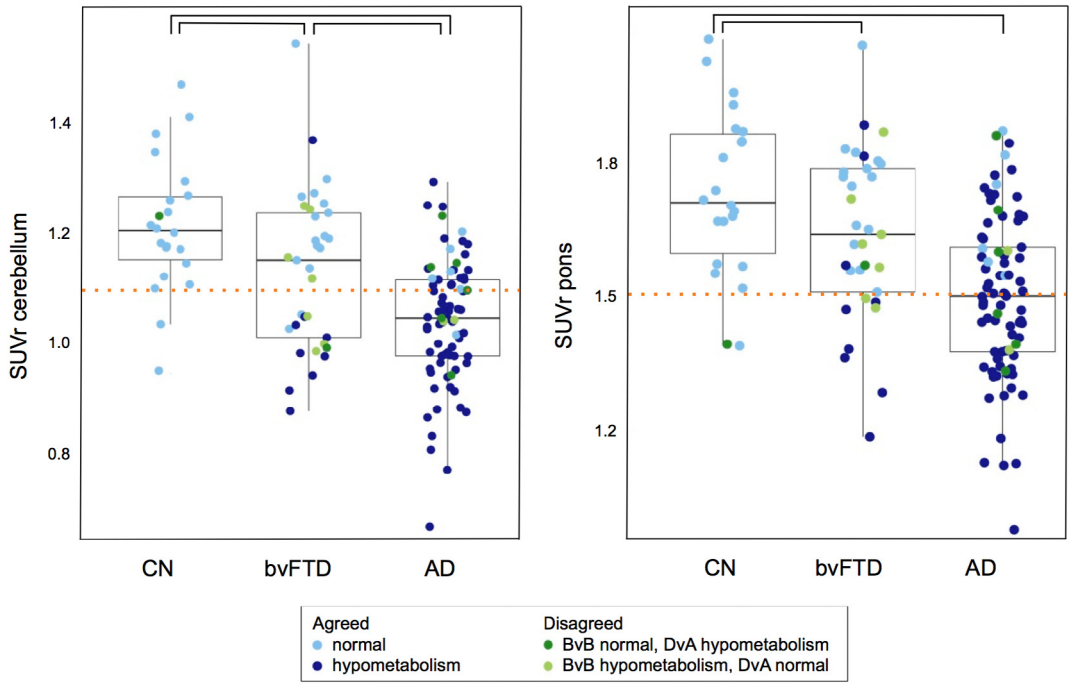

Fig. 2. Boxplots showing PCC [^{18}F]FDG SUVr in CN, bvFTD, and AD with cerebellum (left panel) and pons (right panel) as reference region. Colours indicate whether PCC hypometabolism was present (dark blue) or absent (light blue) as rated by both readers. Green colours indicate disagreement between readers regarding PCC metabolism; light green indicates normal metabolism, and dark green indicates hypometabolism as rated by BvB, where DvA rated metabolism the other way around. The dotted line corresponds with a cut-off defined using the ROC separating PCC [^{18}F]FDG SUVr in AD versus CN.

Table 2
Presence of PCC hypometabolism based on visual reading.

	n	Reader A	reaDer B	κ
All	136	84 (62%)	85 (63%)	0.734
CN	22	1 (5%)	0 (0%)	[a]
bvFTD	33	10 (30%)	16 (49%)	0.509
AD	81	73 (90%)	69 (85%)	0.546

Data are presented in number of patients with PCC hypometabolism (percentage).
[a] κ could not be calculated when reading has resulted in zero patients having PCC hypometabolism.

standardized beta[SE] = 0.263[0.073]), and a negative association with CDR ($p_{interaction}$ = 0.042, eta^2 = 0.264, standardized beta [SE] = −0.434[0.104]). Results are shown in Fig. 5.

4. Discussion

The main finding of this study is that PCC hypometabolism was not restricted to AD, but that it was also present in a substantial part of bvFTD patients based on visual reading and a more data-driven approach. Furthermore, PCC metabolism was positively associated with age and with age at onset of complaints in AD, consistent with an earlier study demonstrating more distinct PCC hypometabolism in early-onset compared with late-onset AD (Rabinovici et al., 2010). Within bvFTD, presence of PCC hypometabolism based on visual reading was associated with worse memory performance. Screening tests for global cognition and dementia severity (i.e. MMSE and CDR) however did not differ from bvFTD patients with normal PCC metabolism. Linear regression analyses revealed that within bvFTD patients with PCC hypometabolism based on visual reading, lower PCC [^{18}F]FDG SUVr was associated with worse memory and visuospatial functioning, as well as with higher scores on the CDR (more severe dementia).

Overall, inter-reader agreement was considered good (κ = 0.734). In bvFTD patients only, however, agreement among readers was considered moderate (κ = 0.509), with presence of PCC hypometabolism ranging from 30 to 49%. Lower inter-reader agreement in bvFTD could be the result of heterogeneity of PCC metabolism, illustrated by a large scatter in Fig. 2, causing increased difficulty in reading. In addition, assignment of PCC hypometabolism depends on metabolism of other brain regions, whereas prominent frontal (or frontotemporal) hypometabolism could increase difficulty or reading in bvFTD. The most experienced reader (reader A) yielded a specificity of 70% for distinguishing AD from bvFTD, comparable with other [^{18}F]FDG-PET studies distinguishing AD from other neurodegenerative disorders, such as Silverman e.a. (73%; Silverman et al., 2001) and Jagust e.a. (74%; Jagust et al., 2007), however worse than Foster e.a. (86%; Foster et al., 2007).

Prevalence of PCC hypometabolism in bvFTD varied using the data-driven approach as well, ranging from 27 to 42%. Prevalence of PCC hypometabolism was highest when the cerebellum was used as reference tissue, coinciding a [^{18}F]FDG SUVr cut-off characterized by higher sensitivity for PCC hypometabolism based on the ROC curve

Table 3
Diagnostic accuracy of SUVr for distinguishing between diagnostic groups.

	ROC-AUC	SUVr cut-off	Specificity	Sensitivity	Positive predictive value	Negative predictive value
CN vs. AD						
SUVr-c	0.86 (0.77–0.96)	1.10	91 (71–99)	70 (59–80)	97 (88–99)	45 (37–54)
SUVr-p	0.81 (0.71–0.91)	1.52	91 (71–99)	56 (44–67)	96 (86–99)	36 (53–72)
CN vs. bvFTD						
SUVr-c	0.66 (0.52–0.81)	1.07	91 (71–99)	42 (25–61)	88 (64–97)	51 (43–59)
SUVr-p	0.64 (0.49–0.79)	1.51	91 (71–99)	27 (13–46)	82 (52–95)	45 (39–52)
bvFTD vs. AD						
SUVr-c	0.68 (0.56–0.80)	0.97	91 (76–98)	23 (15–34)	86 (67–95)	33 (29–36)
SUVr-p	0.71 (0.60–0.82)	1.38	91 (76–98)	30 (20–41)	89 (72–96)	34 (31–39)

Data are presented with 95% confidence intervals. ROC-AUCs were calculated based on continuous SUVr values, with either cerebellum (SUVr-c) or pons (SUVr-p) as reference region. No differences were found when ROC-AUC from pons-normalised data were compared with cerebellum-normalised data using the method by Hanley and McNeil (1983).

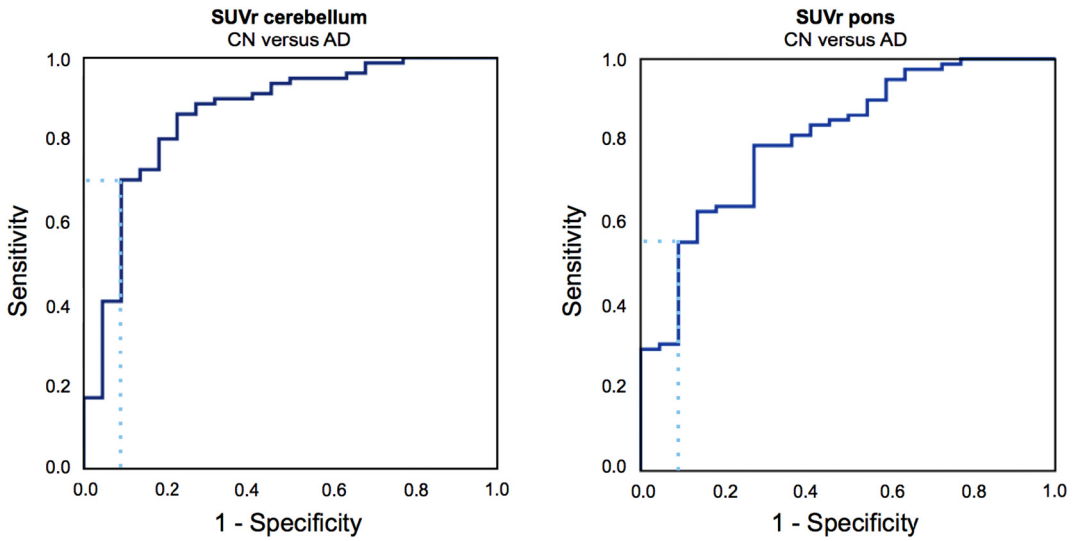

Fig. 3. Receiver operating characteristic separating PCC [^{18}F]FDG SUVr in CN versus AD.

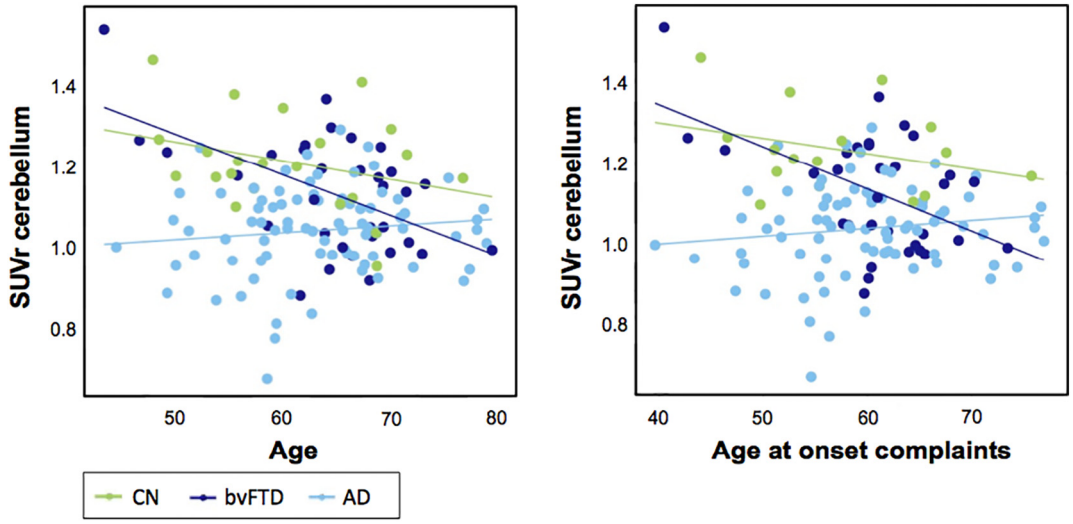

Fig. 4. Linear regression analyses showed associations between PCC [^{18}F]FDG SUVr and age in AD ($p_{interaction}$ = 0.047, standardized beta [SE] = 0.010[0.005]), as well as with age at onset of complaints in AD ($p_{interaction}$ = 0.034, standardized beta[SE] = 0.011[0.055]).

separating AD from CN. Higher ROC classification was found in cerebellum-normalised data compared with pons-normalised data, probably since pons-normalised data has larger scatter, especially in CN subjects and AD patients. Larger scatter in pons-normalised data could be the result of relative better preservation of glucose metabolism in the pons compared with cerebellum in AD (Minoshima et al., 1995).

Table 4
Characteristics of bvFTD patients, divided into subgroups based on absence or presence of PCC hypometabolism.

	n = 33	Normal PCC metabolism n = 23	PCC hypo-metabolism n = 10
PCC metabolism			
[^{18}F]FDG SUVr cerebellum	33	1.18 ± 0.12	1.01 ± 0.14[†]
[^{18}F]FDG SUVr pons	33	1.70 ± 0.14	1.50 ± 0.22[‡]
Demographics			
Age	33	63 ± 8	68 ± 5
Female	33	10 (44)	3 (30)
Education	32	4.5 ± 1.5	4.8 ± 1.3
Duration of complaints	32	3.5 ± 3.2	4.8 ± 3.2
Age at onset complaints	32	60 ± 8	63 ± 5
APOE genotype			
APOE e4 positive		3 (13)	4 (40)
CSF			
Abeta$_{1-42}$ pg/mL	33	924 ± 228	982 ± 263
tau pg/mL	33	349 ± 203	353 ± 200
ptau pg/mL	33	47 ± 17	42 ± 12
Neuropsychological compound z-scores			
Memory	33	0.20 ± 0.57	−0.36 ± 0.69[§]
Language	33	−0.04 ± 0.61	−0.34 ± 0.75
Attention	33	0.05 ± 0.90	−0.12 ± 0.81
Visuospatial functioning	33	0.14 ± 0.50	0.35 ± 0.45
Executive functioning	33	−0.18 ± 0.87	−0.17 ± 1.04
MMSE	33	23.8 ± 3.6	23.3 ± 3.2
CDR	27	0.9 ± 0.6	0.8 ± 0.3
NPI	26	21.9 ± 15.5	15.0 ± 12.4

Assignment of normal PCC metabolism or PCC hypometabolism was based on visual reading by reader A. Data are presented as mean ± standard deviation, or as number (percentage). APOE e4 positive genotype: ≥one e4 alleles. Variables with significant differences on chi-squared tests, Kruskal-Wallis analyses, or ANOVA are indicated as follows.

[†] Difference with normal PCC metabolism $p \leq 0.001$.

[‡] Difference with normal PCC metabolism $p \leq 0.01$.

[§] Difference with normal PCC metabolism $p \leq 0.05$.

Several studies have investigated functional and molecular brain imaging characteristics in AD and bvFTD, but to the best of our knowledge, this is the first study investigating the prevalence and clinical characteristics of hypometabolism in the PCC in a large sample of AD and bvFTD patients at diagnosis. One previous study has investigated PCC hypometabolism in the heterogeneous entity of frontotemporal lobar degeneration, and found hypometabolism in four out of fourteen patients (Womack et al., 2011). Another study separated a sample of eight bvFTD patients based on the presence or absence of autonoetic consciousness, a complex function including the self-awareness in episodic memory, and found that the four impaired patients had lower glucose uptake in the PCC than the others (Bastin et al., 2012). Other studies demonstrated presence of PCC hypometabolism in more advanced disease stages in bvFTD (Broe et al., 2003; Ishii et al., 1998).

A biological explanation for PCC hypometabolism in neurodegenerative diseases might be found in the functional organization of the brain. The PCC is a highly anatomically and functionally connected region in the brain, and an important hub in the default mode network (DMN) (Buckner et al., 2008, 2005; Raichle et al., 2001). AD is characterized by early disruption of the DMN, with prominent involvement of the PCC, whereas bvFTD is most commonly associated with early changes in the salience network (Seeley et al., 2009; Zhou et al., 2010). During disease progression, more brain regions are found to be involved in both AD and bvFTD, suggesting involvement of multiple networks when neurodegeneration progresses. Possibly, involvement of the PCC in bvFTD at diagnosis is associated with further disease progression, supported by our finding that within the subgroup of bvFTD patients with PCC hypometabolism, lower PCC metabolism was associated with worse memory and visuospatial performance, and with greater disease severity based on the CDR score. The suggestion of an association between PCC involvement and further disease severity is consistent with earlier findings (Broe et al., 2003; Ishii et al., 1998). We found no differences, however, between global measurements for disease severity or duration of complaints at baseline when we compared bvFTD patients with PCC hypometabolism with bvFTD patients with normal PCC metabolism. Another hypothesis could be that bvFTD is a highly heterogeneous disorder, associated with a subgroup of patients characterized by PCC involvement already early in the disease, and associated with memory impairment, worse visuospatial functioning, and

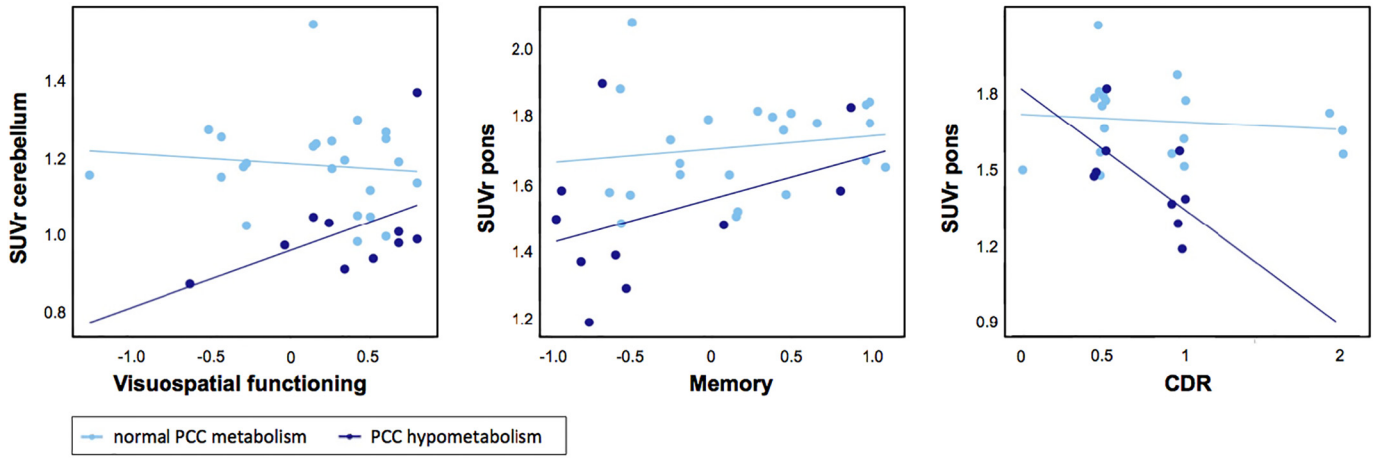

Fig. 5. Linear regression analyses showed associations between PCC [^{18}F]FDG SUVr and visuospatial functioning in bvFTD patients with PCC hypometabolism ($p_{interaction}$ = 0.044, eta^2 = 0.208, standardized beta[SE] = 0.163[0.075]) using cerebellum as reference region, as well as with memory ($p_{interaction}$ = 0.002, eta^2 = 0.419, standardized beta[SE] = 0.263[0.073]), and CDR ($p_{interaction}$ = 0.042, eta^2 = 0.264, standardized beta[SE] = −0.434[0.104]) using the pons as reference region.

more severe dementia when PCC metabolism is lower. An alternative hypothesis could be that local disruption in the frontotemporal cortex affect connected regions such as the PCC in part of the patients (Buckner et al., 2008).

Among the limitations of our study are the relatively small sample sizes, particularly in the CN group. This could have led to less accurate results when the prevalence of PCC metabolism was explored using the PCC [^{18}F]FDG SUVr to define a quantitative cut-off for PCC hypometabolism. Furthermore, the relative small sample size could have resulted in an underestimation of exploratory analyses investigating PCC metabolism with clinical characteristics.

Our findings may have important clinical implications, as [^{18}F]FDG PET is used frequently to differentiate between AD and bvFTD, and especially PCC hypometabolism is commonly considered to be specific for AD. In the differential diagnosis of AD, metabolism of the PCC should be interpreted in the context of different biomarkers, including metabolism of other brain regions and – for example – amyloid and tau status as well.

In conclusion, PCC hypometabolism was present in almost one third of bvFTD patients and therefore it is not restricted to AD. In AD, younger age and age at onset of complaints was associated with lower PCC metabolism, using CN as reference. In addition, within bvFTD patients with PCC hypometabolism based on visual reading, lower PCC metabolism was associated with worse memory and visuospatial functioning, as well as with higher scores on the CDR (more severe dementia).

Supplementary data to this article can be found online at https://doi.org/10.1016/j.nicl.2018.05.024.

Disclosure

Research of the VUmc Alzheimer Center is part of the Neurodegeneration Research program of the Neuroscience Campus Amsterdam.

Acknowledgement

The authors would like to thank the patients, their families, and the cognitive normal subjects for participating in this study.

Compliance with ethical standardsFunding

This study was performed within the framework of CTMM, the Center for Translational Molecular Medicine (www.ctmm.nl), project LeARN (grant 02N-101). This work was also financially supported by the Internationale Stichting Alzheimer Onderzoek (ISAO, grant 05512).

The VUmc Alzheimer Center is supported by Alzheimer Nederland and Stichting VUmc fonds. The clinical database structure was developed with funding from Stichting Dioraphte (VSM-05050700).Conflicts of Interest

N.M.E. Scheltens declares that she has no conflict of interest. K. van der Weijden declares that he has no conflict of interest. Dr. S.M. Adriaanse declares that she has no conflict of interest. P.P. Oomen declares that she has no conflict of interest. Dr. R. Ossenkoppele declares that he has no conflict of interest. W.A. Krudop declares that she has no conflict of interest. Dr. A.A. Lammertsma serves on the editorial boards of European Journal of Nuclear Medicine and Molecular Imaging, Journal of Cerebral Blood Flow and Metabolism, Molecular Imaging and Biology, Oncology Research and Treatment, International Journal of Molecular Imaging, Nuklearmedizin, Clinical and Translational Imaging, American Journal of Nuclear Medicine and Molecular Imaging, Frontiers in Brain Imaging Methods, Journal of Radiology Research and Practice, Current Medical Imaging Reviews and OA Molecular Oncology, and is member of the IFAC BIOMED Technical Committee, the NeuroImaging Committee of the European Association of Nuclear Medicine, and the Board of Appeal of the Dutch Medical Physicist Training Foundation. He has received research grants from Avid, Roche and Philips, and a speaker honorarium from Philips. Dr. F. Barkhof serves as a consultant to Biogen-Idec, Janssen Alzheimer Immunotherapy, Bayer-Schering, Merck-Serono, Roche, Novartis, Genzyme, and Sanofi-aventis. He has received sponsoring from EU-H2020, NWO, SMSR, EU-FP7, TEVA, Novartis, Toshiba, he is supported by the NIHR UCLH biomedical research centre, and he is a member of editorial boards of Radiology, Brain, Neuroradiology, MSJ, and Neurology. T. Koene declares that she has no conflict of interest. Dr. C.E. Teunissen serves on the advisory board of Fujirebio and Roche, received research consumables from Euroimmun, IBL, Fujirebio, Invitrogen and Mesoscale Discovery, and performed contract research for IBL, Shire, Boehringer, Roche and Probiodrug; and received grants from the European Commission, the Dutch Research Council (ZonMW), Association of Frontotemporal Dementia/Alzheimer's Drug Discovery Foundation, ISAO and the Alzheimer's Drug Discovery Foundation. She received research consumables from Euroimmun, IBL, Fujirebio, Invitrogen and Mesoscale Discovery, and performed contract research for IBL, Shire, Boehringer, Roche and Probiodrug. She received lecture fee from Roche and Axon Neurosciences. Dr. Ph. Scheltens has received grant support for the VU University Alzheimer Center from GE Healthcare, Nutricia Research, Piramal and MERCK. In the past 2 years

he has received consultancy/speaker fees (paid to the institution) from Probiodrug, EIP Pharma, Sanofi, Novartis, Piramal and GE Healthcare. Research programs of Wiesje van der Flier have been funded by ZonMW, NWO, EU-FP7, Alzheimer Nederland, CardioVascular Onderzoek Nederland, stichting Dioraphte, Gieskes-Strijbis fonds, Biogen MA Inc., Boehringer Ingelheim, Piramal Neuroimaging, Roche BV, Janssen Stellar, Combinostics. WF has performed contract research for Biogen MA Inc. and Boehringer Ingelheim. WF has been an invited speaker at Boehringer Ingelheim. All funding is paid to her institution. Y.A.L. Pijnenburg declares that she has no conflict of interest. Dr. M. Yaqub declares that he has no conflict of interest. B.N.M. van Berckel receives grant support from ZonMW, ISAO, CTMM, Janssen Pharmaceuticals, GE and AVID radiopharmaceuticalsIn addition he is a trainer for GE and Piramal.Ethical approval

All procedures performed were in accordance with the ethical standards of the institutional and/or national research committee and with the 1964 Helsinki declaration and its later amendments or comparable ethical standards.

References

Bastin, C., Feyers, D., Souchay, C., Guillaume, B., Pepin, J.-L., Lemaire, C., Degueldre, C., Collette, F., Salmon, E., 2012. Frontal and posterior cingulate metabolic impairment in the behavioral variant of frontotemporal dementia with impaired autonoetic consciousness. Hum. Brain Mapp. 33, 1268–1278. http://dx.doi.org/10.1002/hbm.21282.

Broe, M., Hodges, J.R., Schofield, E., Shepherd, C.E., Kril, J.J., Halliday, G.M., 2003. Staging disease severity in pathologically confirmed cases of frontotemporal dementia. Neurology 60, 1005–1011.

Buckner, R.L., Snyder, A.Z., Shannon, B.J., Larossa, G., Sachs, R., Fotenos, A.F., Sheline, Y.I., Klunk, W.E., Mathis, C.A., Morris, J.C., Mintun, M.A., 2005. Molecular, structural, and functional characterization of Alzheimer's disease: evidence for a relationship between default activity, amyloid, and memory. J. Neurosci. 25, 7709–7717. http://dx.doi.org/10.1523/JNEUROSCI.2177-05.2005.

Buckner, R.L., Andrews-Hanna, J.R., Schacter, D.L., 2008. The brain's default network: anatomy, function, and relevance to disease. Ann. N. Y. Acad. Sci. 1124, 1–38. http://dx.doi.org/10.1196/annals.1440.011.

Diehl, J., Grimmer, T., Drzezga, A., Riemenschneider, M., Förstl, H., Kurz, A., 2004. Cerebral metabolic patterns at early stages of frontotemporal dementia and semantic dementia. A PET study. Neurobiol. Aging 25, 1051–1056. http://dx.doi.org/10.1016/j.neurobiolaging.2003.10.007.

Diehl-Schmid, J., Grimmer, T., Drzezga, A., Bornschein, S., Riemenschneider, M., Förstl, H., Schwaiger, M., Kurz, A., 2007. Decline of cerebral glucose metabolism in frontotemporal dementia: a longitudinal 18F-FDG-PET-study. Neurobiol. Aging 28, 42–50. http://dx.doi.org/10.1016/j.neurobiolaging.2005.11.002.

Duits, F.H., Teunissen, C.E., Bouwman, F.H., Visser, P.J., Mattsson, N., Zetterberg, H., Blennow, K., Hansson, O., Minthon, L., Andreasen, N., Marcusson, J., Wallin, A., Rikkert, M.O., Tsolaki, M., Parnetti, L., Herukka, S.-K., Hampel, H., de Leon, M.J., Schröder, J., Aarsland, D., Blankenstein, M.A., Scheltens, P., van der Flier, W.M., 2014. The cerebrospinal fluid "Alzheimer profile": easily said, but what does it mean? Alzheimers Dement. 10, 713–723.e2. http://dx.doi.org/10.1016/j.jalz.2013.12.023.

Foster, N.L., Heidebrink, J.L., Clark, C.M., Jagust, W.J., Arnold, S.E., Barbas, N.R., Decarli, C.S., Turner, R.S., Koeppe, R.A., Higdon, R., Minoshima, S., 2007. FDG-PET improves accuracy in distinguishing frontotemporal dementia and Alzheimer's disease. Brain 130, 2616–2635. http://dx.doi.org/10.1093/brain/awm177.

Hammers, A., Koepp, M.J., Free, S.L., Brett, M., Richardson, M.P., Labbé, C., Cunningham, V.J., Brooks, D.J., Duncan, J., 2002. Implementation and application of a brain template for multiple volumes of interest. Hum. Brain Mapp. 15, 165–174. http://dx.doi.org/10.1002/hbm.10016.

Hanley, J.A., Mcneil, B.J., 1983. A method of comparing the areas under receiver operating characteristic curves derived from the same cases. Radiology 148, 839–843. http://dx.doi.org/10.1148/radiology.148.3.6878708.

Herholz, K., 2014. Guidance for reading FDG PET scans in dementia patients. Q. J. Nucl. Med. Mol. Imaging 58, 332–343.

Ishii, K., Sakamoto, S., Sasaki, M., Kitagaki, H., Yamaji, S., Hashimoto, M., Imamura, T., Shimomura, T., Hirono, N., Mori, E., 1998. Cerebral glucose metabolism in patients with frontotemporal dementia. J. Nucl. Med. 39, 1875–1878.

Jagust, W., Reed, B., Mungas, D., Ellis, W., Decarli, C., 2007. What does fluorodeoxyglucose PET imaging add to a clinical diagnosis of dementia? Neurology 69, 871–877. http://dx.doi.org/10.1212/01.wnl.0000269790.05105.16.

Kato, T., Inui, Y., Nakamura, A., Ito, K., 2016. Brain fluorodeoxyglucose (FDG) PET in dementia. Ageing Res. Rev. 30, 73–84. http://dx.doi.org/10.1016/j.arr.2016.02.003.

Landau, S.M., Harvey, D., Madison, C.M., Koeppe, R.A., Reiman, E.M., Foster, N.L., Weiner, M.W., Jagust, W.J., Alzheimer's Disease Neuroimaging Initiative, 2011. Associations between cognitive, functional, and FDG-PET measures of decline in AD and MCI. Neurobiol. Aging 32, 1207–1218. http://dx.doi.org/10.1016/j.neurobiolaging.2009.07.002.

Loessner, A., Alavi, A., Lewandrowski, K.U., Mozley, D., Souder, E., Gur, R.E., 1995. Regional cerebral function determined by FDG-PET in healthy volunteers: normal patterns and changes with age. J. Nucl. Med. 36, 1141–1149.

Mckhann, G.M., Knopman, D.S., Chertkow, H., Hyman, B.T., Jack, C.R., Kawas, C.H., Klunk, W.E., Koroshetz, W.J., Manly, J.J., Mayeux, R., Mohs, R.C., Morris, J.C., Rossor, M.N., Scheltens, P., Carrillo, M.C., Thies, B., Weintraub, S., Phelps, C.H., 2011. The diagnosis of dementia due to Alzheimer's disease: recommendations from the National Institute on Aging-Alzheimer's Association workgroups on diagnostic guidelines for Alzheimer's disease. Alzheimers Dement. 263–269. http://dx.doi.org/10.1016/j.jalz.2011.03.005.

Minoshima, S., Koeppe, R.A., Frey, K.A., Ishihara, M., Kuhl, D.E., 1994. Stereotactic PET atlas of the human brain: aid for visual interpretation of functional brain images. J. Nucl. Med. 35, 949–954.

Minoshima, S., Frey, K.A., Foster, N.L., Kuhl, D.E., 1995. Preserved pontine glucose metabolism in Alzheimer disease: a reference region for functional brain image (PET) analysis. J. Comput. Assist. Tomogr. 19, 541–547.

Minoshima, S., Giordani, B., Berent, S., Frey, K.A., Foster, N.L., Kuhl, D.E., 1997. Metabolic reduction in the posterior cingulate cortex in very early Alzheimer's disease. Ann. Neurol. 42, 85–94. http://dx.doi.org/10.1002/ana.410420114.

Mulder, C., Verwey, N.A., van der Flier, W.M., Bouwman, F.H., Kok, A., van Elk, E.J., Scheltens, P., Blankenstein, M.A., 2010. Amyloid-beta(1-42), total tau, and phosphorylated tau as cerebrospinal fluid biomarkers for the diagnosis of Alzheimer disease. Clin. Chem. 56, 248–253. http://dx.doi.org/10.1373/clinchem.2009.130518.

Rabinovici, G.D., Furst, A.J., Alkalay, A., Racine, C.A., O'Neil, J.P., Janabi, M., Baker, S.L., Agarwal, N., Bonasera, S.J., Mormino, E.C., Weiner, M.W., Gorno-Tempini, M.L., Rosen, H.J., Miller, B.L., Jagust, W.J., 2010. Increased metabolic vulnerability in early-onset Alzheimer's disease is not related to amyloid burden. Brain 133, 512–528. http://dx.doi.org/10.1093/brain/awp326.

Raichle, M.E., Macleod, A.M., Snyder, A.Z., Powers, W.J., Gusnard, D.A., Shulman, G.L., 2001. A default mode of brain function. Proc. Natl. Acad. Sci. U. S. A. 98, 676–682. http://dx.doi.org/10.1073/pnas.98.2.676.

Rascovsky, K., Hodges, J.R., Knopman, D., Mendez, M.F., Kramer, J.H., Neuhaus, J., van Swieten, J.C., Seelaar, H., Dopper, E.G.P., Onyike, C.U., Hillis, A.E., Josephs, K.A., Boeve, B.F., Kertesz, A., Seeley, W.W., Rankin, K.P., Johnson, J.K., Gorno-Tempini, M.-L., Rosen, H., Prioleau-Latham, C.E., Lee, A., Kipps, C.M., Lillo, P., Piguet, O., Rohrer, J.D., Rossor, M.N., Warren, J.D., Fox, N.C., Galasko, D., Salmon, D.P., Black, S.E., Mesulam, M., Weintraub, S., Dickerson, B.C., Diehl-Schmid, J., Pasquier, F., Deramecourt, V., Lebert, F., Pijnenburg, Y., Chow, T.W., Manes, F., Grafman, J., Cappa, S.F., Freedman, M., Grossman, M., Miller, B.L., 2011. Sensitivity of revised diagnostic criteria for the behavioural variant of frontotemporal dementia. Brain 134, 2456–2477. http://dx.doi.org/10.1093/brain/awr179.

Seeley, W.W., Crawford, R.K., Zhou, J., Miller, B.L., Greicius, M.D., 2009. Neurodegenerative diseases target large-scale human brain networks. Neuron 62, 42–52. http://dx.doi.org/10.1016/j.neuron.2009.03.024.

Silverman, D.H., Small, G.W., Chang, C.Y., Lu, C.S., Kung De Aburto, M.A., Chen, W., Czernin, J., Rapoport, S.I., Pietrini, P., Alexander, G.E., Schapiro, M.B., Jagust, W.J., Hoffman, J.M., Welsh-Bohmer, K.A., Alavi, A., Clark, C.M., Salmon, E., de Leon, M.J., Mielke, R., Cummings, J.L., Kowell, A.P., Gambhir, S.S., Hoh, C.K., Phelps, M.E., 2001. Positron emission tomography in evaluation of dementia: regional brain metabolism and long-term outcome. JAMA 286, 2120–2127.

Svarer, C., Madsen, K., Hasselbalch, S.G., Pinborg, L.H., Haugbøl, S., Frøkjaer, V.G., Holm, S., Paulson, O.B., Knudsen, G.M., 2005. MR-based automatic delineation of volumes of interest in human brain PET images using probability maps. NeuroImage 24, 969–979. http://dx.doi.org/10.1016/j.neuroimage.2004.10.017.

van der Flier, W.M., Pijnenburg, Y.A.L., Prins, N., Lemstra, A.W., Bouwman, F.H., Teunissen, C.E., van Berckel, B.N.M., Stam, C.J., Barkhof, F., Visser, P.J., van Egmond, E., Scheltens, P., 2014. Optimizing patient care and research: the Amsterdam Dementia Cohort. J. Alzheimers Dis. 41, 313–327. http://dx.doi.org/10.3233/JAD-132306.

Verfaillie, S.C.J., Adriaanse, S.M., Binnewijzend, M.A.A., Benedictus, M.R., Ossenkoppele, R., Wattjes, M.P., Pijnenburg, Y.A.L., van der Flier, W.M., Lammertsma, A.A., Kuijer, J.P.A., Boellaard, R., Scheltens, P., van Berckel, B.N.M., Barkhof, F., 2015. Cerebral perfusion and glucose metabolism in Alzheimer's disease and frontotemporal dementia: two sides of the same coin? Eur. Radiol. 1–10. http://dx.doi.org/10.1007/s00330-015-3696-1.

Whitwell, J.L., Anderson, V.M., Scahill, R.I., Rossor, M.N., Fox, N.C., 2004. Longitudinal patterns of regional change on volumetric MRI in frontotemporal lobar degeneration. Dement. Geriatr. Cogn. Disord. 17, 307–310. http://dx.doi.org/10.1159/000077160.

Womack, K.B., Diaz-Arrastia, R., Aizenstein, H.J., Arnold, S.E., Barbas, N.R., Boeve, B.F., Clark, C.M., Decarli, C.S., Jagust, W.J., Leverenz, J.B., Peskind, E.R., Turner, R.S., Zamrini, E.Y., Heidebrink, J.L., Burke, J.R., Dekosky, S.T., Farlow, M.R., Gabel, M.J., Higdon, R., Kawas, C.H., Koeppe, R.A., Lipton, A.M., Foster, N.L., 2011. Temporoparietal hypometabolism in frontotemporal lobar degeneration and associated imaging diagnostic errors. Arch. Neurol. 68, 329–337. http://dx.doi.org/10.1001/archneurol.2010.295.

Zhou, J., Greicius, M.D., Gennatas, E.D., Growdon, M.E., Jang, J.Y., Rabinovici, G.D., Kramer, J.H., Weiner, M., Miller, B.L., Seeley, W.W., 2010. Divergent network connectivity changes in behavioural variant frontotemporal dementia and Alzheimer's disease. Brain 133, 1352–1367. http://dx.doi.org/10.1093/brain/awq075.

Zwan, M.D., Ossenkoppele, R., Tolboom, N., Beunders, A.J.M., Kloet, R.W., Adriaanse, S.M., Boellaard, R., Windhorst, A.D., Raijmakers, P., Adams, H., Lammertsma, A.A., Scheltens, P., van der Flier, W.M., van Berckel, B.N.M., 2014. Comparison of simplified parametric methods for visual interpretation of 11C-Pittsburgh compound-B PET images. J. Nucl. Med. 55, 1305–1307. http://dx.doi.org/10.2967/jnumed.114.139121.